Expanded View Figures

Figure EV1. Polymerizing hGBP1$_F$ binds directly to *Shigella flexneri* across a physiological range of hGBP1$_F$ protein concentrations.

A Time-lapse microscopy frames of formaldehyde-fixed GFP$^+$ *S. flexneri* following admixture of varying concentrations of Alexa-Fluor647-labeled hGBP1$_F$ and 2 mM GTP. Individual time frames depict hGBP1$_F$ fluorescence intensity. Merged images of hGBP1$_F$ and *S. flexneri* fluorescence are shown for the 60 min time points.

B Polymerization of 10 μM hGBP1$_F$ monitored over time by absorption spectroscopy at 350 nm after addition of 2 mM (GTP, GppNHp, GTPγS) or 250 μM (GDP·AlF$_X$) nucleotide.

C Confocal images taken of formaldehyde-fixed GFP$^+$ *S. flexneri* and rhodamine-labeled lipid vesicles 20 min after addition of 10 μM Alexa-Fluor647-hGBP1$_F$ and 2 mM GTP, 2 mM GTPγS, or 250 μM GDP·AlF$_X$.

D Model: In its GTP-bound conformation, the C-terminal farnesyl tail is released from its hydrophobic pocket allowing hGBP1 to bind to lipid vesicles *in vitro* and to host membranes inside human cells. Direct binding to bacteria on the other hand requires hGBP1 to self-assemble over several GTP turnover cycles into polymers. These hGBP1 polymers bind to *S. flexneri* directly and then transition into a bacteria-encapsulating protein coat.

Data information: All scale bars equal 5 μm.

Source data are available online for this figure.

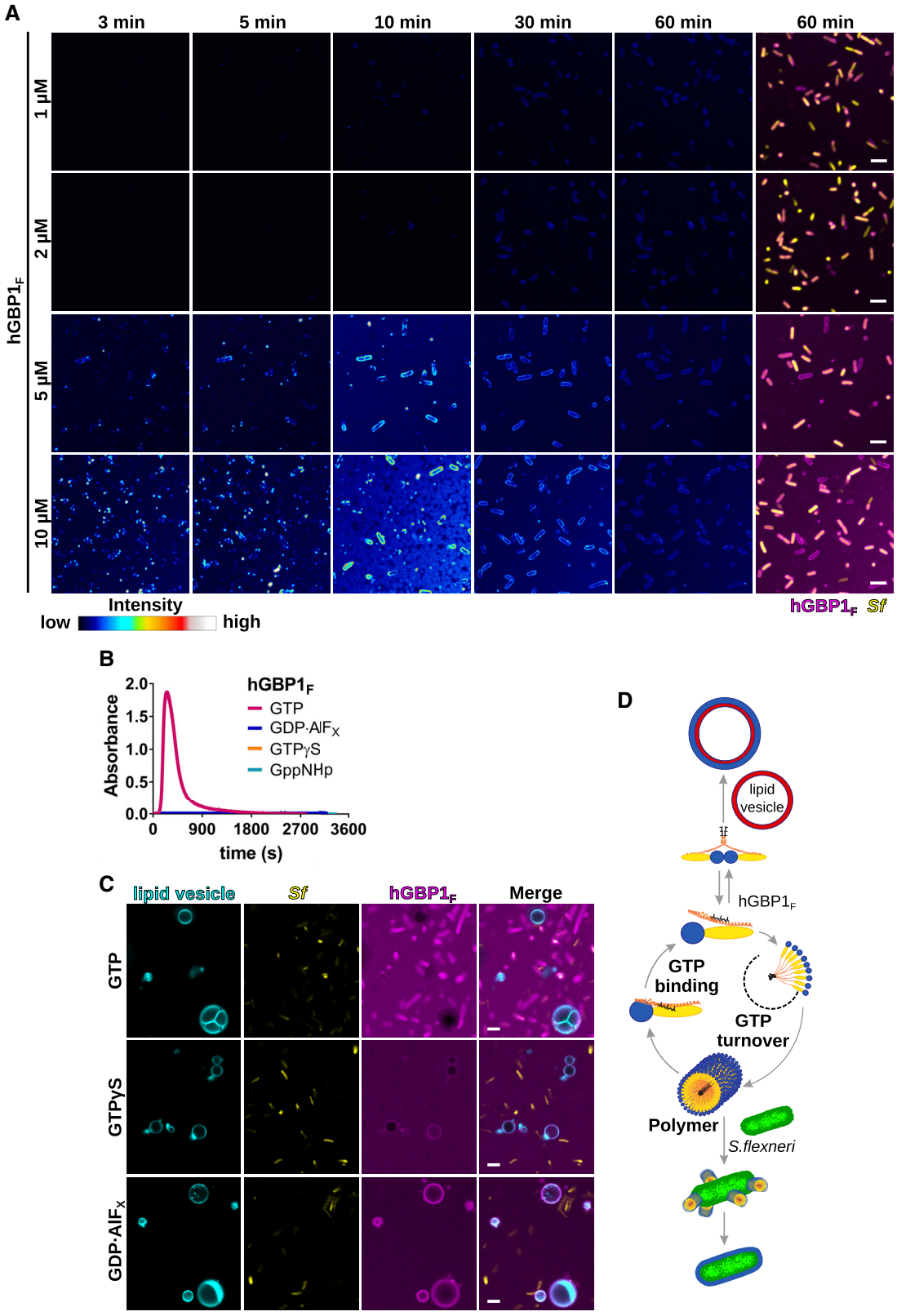

Figure EV1.

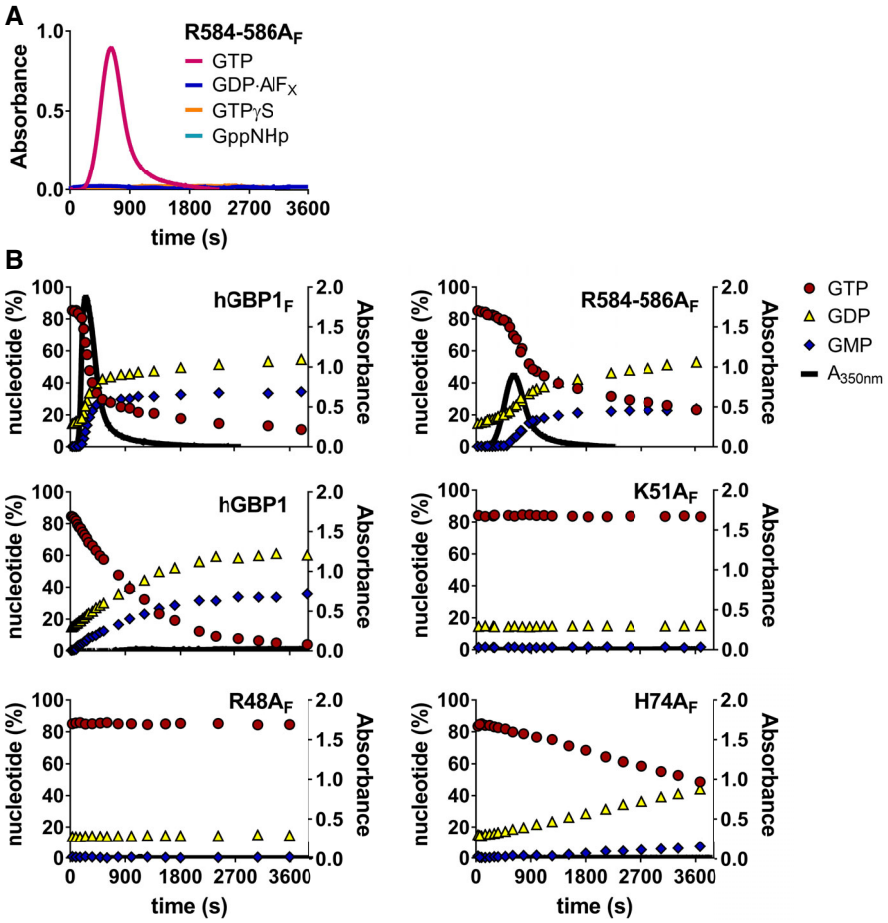

C

turnover number±SEM (min^{-1})		
hGBP1$_F$	3±1	(1st phase)
hGBP1$_F$	29±4	(2nd phase)
R584-586A$_F$	2.2±0.3	(1st phase)
R584-586A$_F$	12±3	(2nd phase)
hGBP1	6.9±0.4	
R584-586A	5.7±0.5	
K51A$_F$	0.013±0.006	
R48A$_F$	0.036±0.007	
H74A$_F$	1.18±0.03	

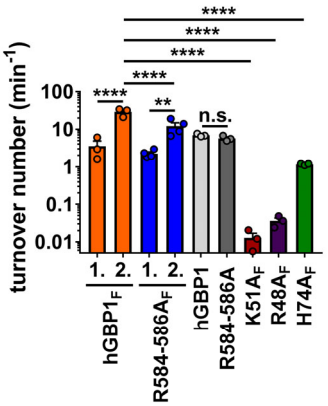

Figure EV2. hGBP1$_F$ polymerization is dependent on GTP, and subsequent GDP hydrolysis and its dynamics are modified by the C-terminal 3R stretch.

A Polymerization of 10 μM hGBP1$_F^{R584\text{-}586A}$ was monitored over time by absorption spectroscopy at 350 nm after admixture of 2 mM (GTP, GppNHp, GTPγS) or 250 μM (GDP·AlF$_X$) nucleotide.

B Polymerization of different hGBP1 variants (at 10 μM) induced by 2 mM GTP was monitored over time by absorption spectroscopy at 350 nm. Absorbance signals were superimposed with nucleotide composition analyzed at defined time points of the corresponding sample. Blots for hGBP1$_F$ and hGBP1$_F^{R584\text{-}586A}$ are the same as shown in Fig 3A.

C GTP turnover numbers were determined for different hGBP1 variants. Turnover numbers for both the slow and the fast phases of GTP hydrolysis (1st phase [1.], 2nd phase [2.]) were quantified during hGBP1$_F$ and hGBP1$_F^{R584\text{-}586A}$ polymerization. Combined data from three independent experiments are shown as mean turnover numbers ± SEM. Significance was determined by two-way ANOVA with Tukey's multiple comparison test. n.s., not significant; $^{**}P \leq 0.01$; $^{****}P \leq 0.0001$.

Source data are available online for this figure.

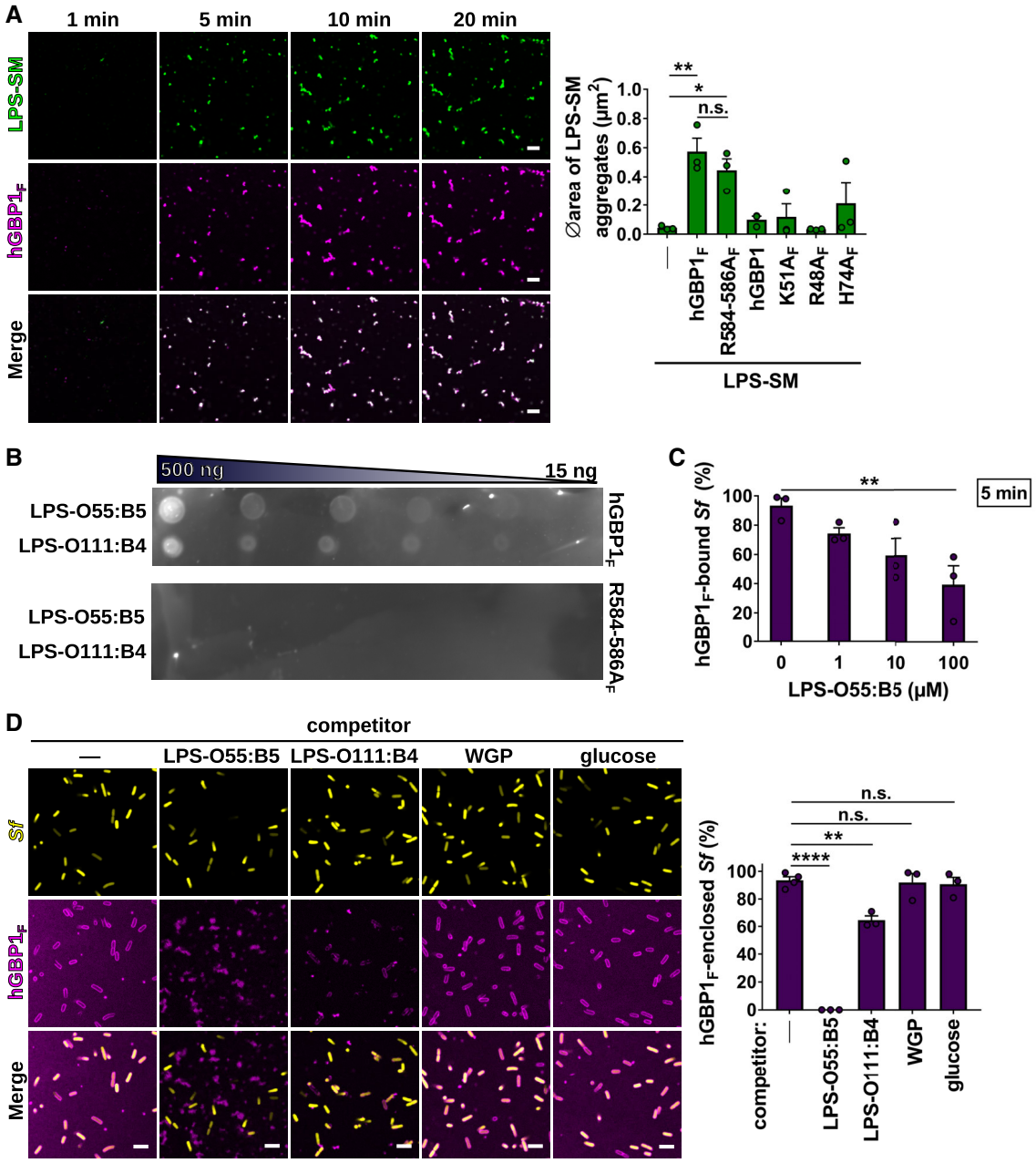

Figure EV3. Polymerizing hGBP1$_F$ binds to and clusters LPS, which acts as a competitive inhibitor blocking hGBP1$_F$ encapsulation of *Shigella flexneri*.

A Confocal time-lapse microscopy frames of 5 µM Alexa-Fluor488-LPS derived from *Salmonella minnesota* (LPS-SM) mixed with 5 µM Alexa-Fluor647-hGBP1$_F$ in the presence of 2 mM GTP. Graph depicts average aggregate area of Alexa-Fluor488-LPS-SM supplemented with 2 mM GTP and 5 µM of the indicated hGBP1 variant. Mean area ± SEM of combined data from three independent experiments. Significance was determined by one-way ANOVA with Tukey's multiple comparison test. n.s., not significant; *$P \leq 0.05$; **$P \leq 0.01$.

B Nitrocellulose membrane dotted with 15–500 ng LPS-O55:B5 and LPS-O111:B4 spots was incubated with 2 µM Alexa-Fluor647-hGBP1$_F$ or Alexa-Fluor647-hGBP1$_F^{R584-586A}$ for 10 min in the presence of 1 mM GTP before measuring fluorescent signals.

C Percentage of hGBP1$_F$-bound formaldehyde-fixed GFP$^+$ *S. flexneri* after 5 min of incubation with 5 µM hGBP1$_F$ and 2 mM GTP in the presence of the indicated concentrations of LPS-O55:B5. Mean percentages ± SEM of combined data from three independent experiments are shown. Significance was determined by one-way ANOVA with Tukey's multiple comparison test. **$P \leq 0.01$.

D Confocal images of formaldehyde-fixed GFP$^+$ *S. flexneri* supplemented with different carbohydrate species (LPS-O55:B5, LPS-O111:B4, glucose—100 µM; whole glucan particles (WGP) 1 mg/ml) taken 60 min after addition of 5 µM Alexa-Fluor647-hGBP1$_F$ and 2 mM GTP. After 60 min of incubation time, hGBP1$_F$-enclosed bacteria were quantified. Mean frequencies ± SEM of combined data from three independent experiments are shown. Significance was determined by one-way ANOVA with Tukey's multiple comparison test. n.s., not significant; **$P \leq 0.01$; ****$P \leq 0.0001$.

Data information: All scale bars equal 5 µm.

Source data are available online for this figure.

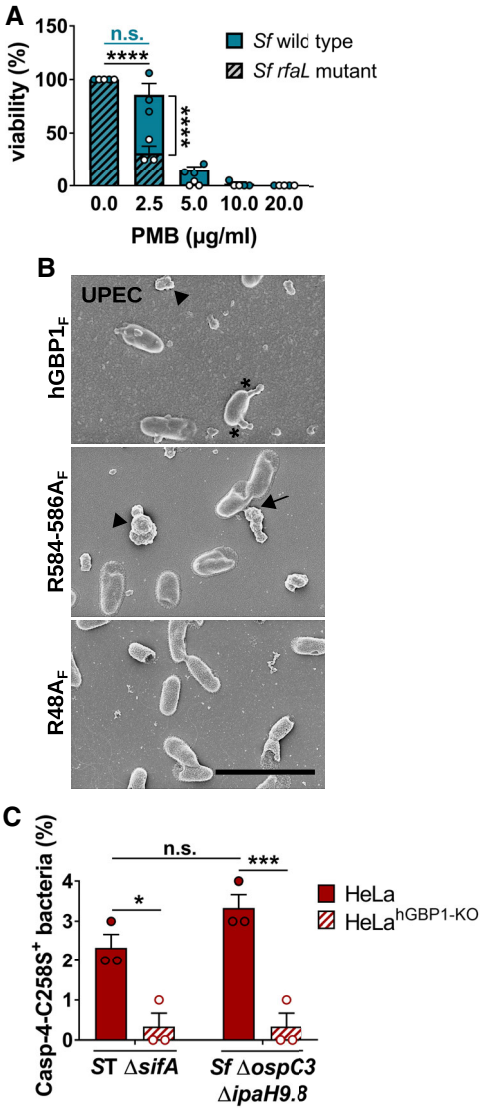

Figure EV4. Lack of O-antigen renders *Shigella flexneri* more susceptible to polymyxin B.

A Following incubation for 45 min with buffer, live *S. flexneri* wild type and *rfaL* mutant were treated for 30 min with varying concentrations of polymyxin B (PMB). The number of viable bacteria was subsequently determined by CFU counts. Graphs show mean CFUs ± SEM of combined data from three independent experiments. Significance was determined by two-way ANOVA with Tukey's multiple comparison test. n.s., not significant; ****$P \leq 0.0001$.

B Scanning electron micrographs of live UPEC incubated for 4 min with 5 µM $hGBP1_F$ or equivalent concentration of either $hGBP1_F^{R584\text{-}586A}$ or $hGBP1_F^{R48A}$ in the presence of 2 mM GTP. Scale bar equals 5 µm. Arrowheads point to unattached hGBP1 polymers, arrows point to hGBP1 polymers attached to bacteria, and asterisks mark polymeric structures that appear to fuse with bacterial surfaces.

C IFNγ-primed wild type and hGBP1-KO HeLa cells stably expressing YFP-Caspase-4^{C258S} were infected with either *Salmonella enterica* Typhimurium mutant Δ*sifA* (MOI = 25) or with *S. flexneri* Δ*ospC3*Δ*ipaH9.8* (MOI = 6). Cells were fixed at 4 hpi (ST Δ*sifA*) or at 2 hpi (*Sf* Δ*ospC3*Δ*ipaH9.8*). Percentage of YFP-Caspase-4^{C258S}-associated bacteria were quantified, and mean ± SEM of combined data from three independent experiments are shown. Significance was determined by two-way ANOVA with Tukey's multiple comparison test. n.s., not significant; *$P \leq 0.05$; ***$P \leq 0.001$.

Source data are available online for this figure.

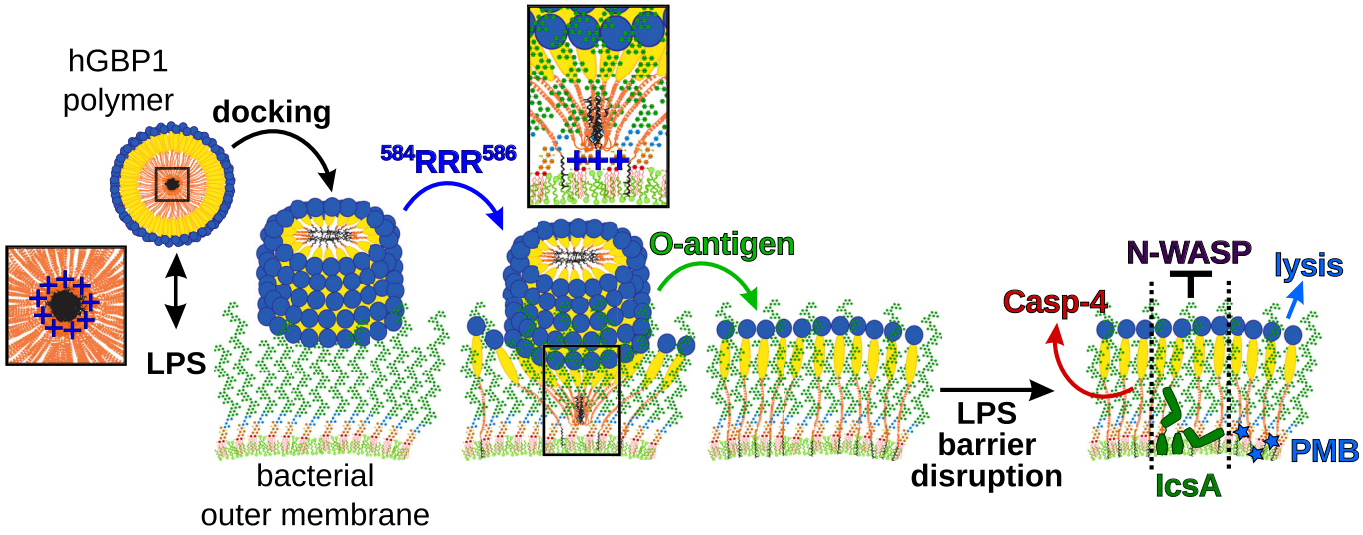

Figure EV5. Model: hGBP1 acts as an LPS-binding surfactant and thereby exerts pleiotropic effects on the functionality of gram-negative bacterial cell envelopes.

Model: Polymerizing hGBP1 binds to LPS and docks to the surface of gram-negative bacteria. The C-termini of polymerized hGBP1 molecules contain three arginines (^{584}RRR^{586}, 3R stretch) which form a positively charged ring around the polymer's hydrophobic core. This positively charged ring promotes stable binding of hGBP1 polymers to the bacterial surface through two non-mutually exclusive mechanisms: (i) attractive electrostatic interactions between hGBP1's C-terminal 3R stretch and negative charges on the surface of the bacterial outer membrane (phosphate groups present at the inner core and lipid A segments of LPS) pull the polymer's hydrophobic core toward the bacterial membrane; and (ii) accelerated depolymerization releases the farnesyl tails from the polymer's hydrophobic core to anchor farnesylated hGBP1 inside the outer leaflet of bacterial outer membranes. The depolymerization process leads to the formation of a seemingly uniform hGBP1 protein coat encasing entire bacteria. The transition from docked hGBP1 polymers into a stable hGBP1 protein coat is dependent on O-antigen, the outer polysaccharide structure of bacterial LPS. We propose that interactions with O-antigen maintain individual hGBP1 molecules in their outstretched conformation, as these proteins become anchored inside the bacterial outer membrane via their farnesyl tails. Inserted hGBP1 polymers as well as embedded individual hGBP1 proteins act as surfactants and disrupt LPS barrier functions. By clustering LPS molecules together, hGBP1 exerts pleiotropic effects on the functionality of gram-negative bacterial cell envelopes: Binding of hGBP1 to the bacterial surface unmasks lipid A for attack by caspase-4 or the antimicrobial peptide polymyxin B. The "detergent-like" activity of hGBP1 further disturbs the polar localization and O-antigen-dependent function of the *Shigella* virulence protein IcsA, thereby interfering with the pathogen's ability to form actin tails required for bacterial dissemination.